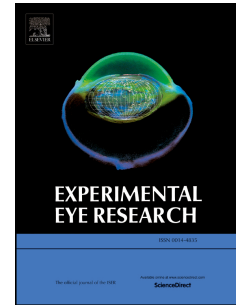# Journal Pre-proof

Depth-dependent mechanical properties of the human cornea by uniaxial extension

Malavika H. Nambiar, Theo G. Seiler, Sebastian Senti, Layko Liechti, Fabian Müller, Harald Studer, Abhijit S. Roy, Philippe Büchler

Please cite this article as: Nambiar, M.H., Seiler, T.G., Senti, S., Liechti, L., Müller, F., Studer, H., Roy, A.S., Büchler, P., Depth-dependent mechanical properties of the human cornea by uniaxial extension, *Experimental Eye Research* (2023), doi: https://doi.org/10.1016/j.exer.2023.109718.

This is a PDF file of an article that has undergone enhancements after acceptance, such as the addition of a cover page and metadata, and formatting for readability, but it is not yet the definitive version of record. This version will undergo additional copyediting, typesetting and review before it is published in its final form, but we are providing this version to give early visibility of the article. Please note that, during the production process, errors may be discovered which could affect the content, and all legal disclaimers that apply to the journal pertain.

Depth-dependent mechanical properties of the human cornea by uniaxial extension

Malavika H. Nambiar[1], Theo G. Seiler[2,3,4], Sebastian Senti[1], Layko Liechti[5], Fabian Müller[5] Harald Studer, Abhijit S. Roy[6], Philippe Büchler[1]

1. ARTORG Center for Biomedical Engineering Research, University of Bern, Freiburgstrasse 3, 3010 Bern, Switzerland

2. IROC AG, Institut für Refraktive und Ophthalmo-Chirurgie, Stockerstrasse 37, 8002 Zürich, Switzerland

3. Universitätsklinik für Augenheilkunde, Inselspital Bern, Freiburgstrasse 15, 3010 Bern, Switzerland

4. Klinik für Augenheilkunde, Universitätsklinikum Düsseldorf, Moorenstr. 5, 40225 Düsseldorf, Deutschland

5. Ziemer Ophthalmic Systems AG, Allmendstrasse 11, 2562 Port, Switzerland

6. Narayana Nethralaya Eye Clinic, Bengaluru, Karnataka 560010, India

Malavika H. Nambiar – malavika.nambiar@unibe.ch

Theo G. Seiler – theo@seiler.tv

Sebastian Senti – Sebastian.senti@unibe.ch

Layko Liechti – Layko.Liechti@ziemergroup.com

Fabian Müller – fabian.mueller@ziemergroup.com

Harald Studer – harald.studer@gmail.com

Abhijit S. Roy – asroy27@yahoo.com

Philippe Büchler – philippe.buechler@unibe.ch

25   **ABSTRACT**

26   The purpose of this study was to investigate the depth-dependent biomechanical properties of the

27   human corneal stroma under uniaxial tensile loading. Human stroma samples were obtained after the

28   removal of Descemet's membrane in the course of Descemet's membrane endothelial keratoplasty

29   (DMEK) transplantation. Uniaxial tensile tests were performed at three different depths: anterior,

30   central, and posterior on 2 x 6 x 0.15 mm strips taken from the central DMEK graft. The measured

31   force-displacement data were used to calculate stress-strain curves and to derive the tangent

32   modulus. The study showed that mechanical strength decreased significantly with depth. The anterior

33   cornea appeared to be the stiffest, with a stiffness approximately 18% higher than that of the central

34   cornea and approximately 38% higher than that of the posterior layer. Larger variations in mechanical

35   response were observed in the posterior group, probably due to the higher degree of alignment of the

36   collagen fibers in the posterior sections of the cornea. This study contributes to a better understanding

37   of the biomechanical tensile properties of the cornea, which has important implications for the

38   development of new treatment strategies for corneal diseases. Accurate quantification of tensile

39   strength as a function of depth is critical information that is lacking in human corneal biomechanics to

40   develop numerical models and new treatment methods.

41

43   **1. INTRODUCTION**

44   Over 185,000 corneal transplant surgeries are performed annually worldwide, yet, 53% of the world's

45   population does not have access to donor corneas, which also limits their availability for research

46   (Bunya et al., 2023). Understanding the biomechanical properties of the cornea can help us develop

47   more effective surgical interventions and treatment strategies that can restore corneal integrity and

48   prevent the progression of corneal diseases. It is critical to understand the biomechanics of this

49   complex tissue, which is highly anisotropic, heterogeneous, and multi-layered. Knowledge of the

50   tensile strength of the cornea can help improve treatment strategies for conditions that affect the

51   structural integrity of the cornea, such as keratoconus, corneal ectasia, and corneal ulcers. For

52   example, measuring corneal resistance to deformation or stress can help us determine the optimal

53   parameters for corneal crosslinking to strengthen corneal tissue in keratoconus, or design

54   keratotomies to appropriately reduce corneal astigmatism. In addition, studying the tensile strength

55   of corneal tissue can also contribute to the development of new biomaterials, implants and surgical

56   techniques for corneal reconstruction and transplantation (Roberts, 2016).

57   While full-thickness tensile testing has been performed on human corneal strips (Elsheikh et al., 2008;

58   Hoeltzel et al., 1992; Mahdian et al., 2021), there is limited information in the literature on the depth-

59   dependent biomechanics of the human cornea, particularly on tensile properties. Existing studies on

60   depth dependence have been performed using shear (Petsche et al., 2012; Sloan et al., 2014),

61   compression (Ramirez-Garcia et al., 2018), cohesive tension (Randleman et al., 2008), and indentation

62   (Labate et al., 2015) methods. Physiologically, however, the cornea is subjected to tension due to the

63   intraocular pressure, which is most important for understanding its biomechanics.

64   Therefore, this study aims to characterize the mechanical properties of the human corneal stroma at

65   different depths, corresponding to the anterior, central, and posterior corneal stroma by uniaxial

66   extension. To our knowledge, this is the first depth-dependent uniaxial tensile study performed on

67   human corneas. To control sample preparation, strips were cut with a femtosecond laser to ensure

68   uniform geometry and thickness and to precisely control the depth of sample extraction.

69

70   **MATERIALS AND METHODS**

71   **2.1 Experimental setup**

72   Nine human donor corneas (age 55-79 years) were examined in this study. Since good quality corneal

73   tissue is scarce, this study used corneas after the removal of Descemet's membrane (DM) for DMEK

74   surgery. The corneas including a 3 mm scleral ring, were provided by the Department of

75   Ophthalmology of the Inselspital Bern immediately after peeling the DM, which was performed

76   without damaging the posterior corneal stroma. Before DM peeling, the corneas were examined for

77   corneal scars and de-swollen in Carry-C (Alchimia, Italy) for 24 hours. After DM peeling, the corneas

78   were placed in a hydration preserving culture medium containing 5 % Dextran solution. Since this

79   study used tissue from decreased donors that would otherwise be discarded, the IRB (Cantonal Ethics

80   Committee of the Canton of Bern) granted exempt status. The orientation of the corneas were

81   unknown.

82   Within 72 hours after DM peeling, the cornea was placed in an artificial anterior chamber

83   pressurization device with the corneal epithelium side facing upward to prevent movement during

84   strip cutting with the Femto LDV Z8 Neo femtosecond laser (Ziemer Ophthalmic Systems AG,

85   Switzerland) (Figure 1). The laser handpiece was centered on the cornea using the OCT integrated into

86   the device and moved only after all strips were cut. The OCT was also used to measure the total corneal

87   thickness. The average central corneal thickness in this study was 770 µm. The high thickness variation

88   can be attributed to swelling, despite the deswelling media due to lack of the endothelium layer. For

89   each eye, three strips 6 mm long, 2 mm wide, and 0.15 mm thick were cut in the central-corneal region

90   from the anterior (D1), central (D2), and posterior (D3) thirds of the cornea. No epithelium was present

91   on the prepared samples. In all but two samples, the first 100 µm of cornea were discarded to ensure

92   that the Bowmann's membrane was not included in the test. In the two excluded samples, it was not

93   possible to omit this layer because of low corneal thickness, so the anterior sample (D1) was taken

94   just below the epithelium. However, no differences were observed in the tests. The samples were

95   individually preserved and tested in a hydration-preserving culture medium containing 5 % Dextran to

96   maintain the sample dimensions after cutting (Hamon et al., 2021; Wolf et al., 2009).

97   The strips were uniaxially tested in a bath containing the same culture medium using the Ustretch

98   device (CellScale, Waterloo, Canada) at room temperature (Figure 2). The tissue was pre-stretched

99   with a low force of 10 mN to ensure uniform tension across the samples. The samples were then

100   loaded with 6 cycles at a strain rate of 0.16 % /s. The fifth cycle of force-displacement data was

101   recorded for analysis as the mechanical response of the tissue stabilized after the fifth preconditioning

102   cycle. The specimens were tested up to a strain of 10 %, which is consistent with previous experiments

103   (Boschetti et al., 2012; Elsheikh et al., 2011, 2008; Wollensak et al., 2003). The actual length of the

104   specimen was used to calculate the strain, taking into account the distance between the grips under

105   the pre-stretch 10 mN, which differs from the original distance of 5 mm due to the initial tensioning

106   of the testing device and the unfolding of the specimen. For this reason, the reference length of the

107   sample was calculated as the actual distance of the grip at the start of the 5th cycle. The strain was

108   then calculated as the ratio of extension to this reference length of the sample. The stress was

109   determined by dividing the force by the original cross-sectional area, specifically the product of the

110   thickness of the sample (0.15 mm) and the width at the attachment of the rakes (1.56 mm).

111   The relationship between stress and strain was further characterized using an exponential function

112   based on a previously proposed method for studying corneal inflation (Eliasy et al., 2019; Elsheikh et

113   al., 2010):

$$\sigma = A\big(e^{B(\varepsilon - \varepsilon_0)} - 1\big) \tag{1}$$

115   Here, A and B are material parameters, and ε_0 is determined such that the stress corresponds to our

116   experimental measurement at zero strain. This additional strain is necessary to account for the initial

117   experimental pre-stress introduced to remove the initial compliance of the measurement setup.

118   Finally, the stiffness of the specimen was calculated as the derivative of the fitted exponential function

119   and used to quantify the stiffness ratio between the different depths.

120 **2.2 Statistical Methods**

121 Statistical analysis was performed using Python 3.7 (Scipy.stats). The uniaxial force and extension data

122 were used to generate stress-strain curves for each depth and sample. Tangent moduli were

123 calculated for the low (2 %), intermediate (5 %), and high-strain (10 %) regions of the curves,

124 corresponding to the stiffness of the tissue at different depths. A one-way ANOVA was performed on

125 the tangent moduli data for each depth group to analyze the difference between depths. Due to

126 sample exclusion during experimental measurements, our sample size was insufficient to perform

127 paired statistical tests. A Tukey post hoc test was used to determine which groups were significantly

128 different. A p-value of < 0.05 was considered significant.

129   ## 2. RESULTS

130   Twenty-seven strips were cut from the 9 donor corneas, but 4 strips were excluded from analysis,

131   bringing the total number of samples for all groups to 23. The main reason for exclusion was damage

132   to the sample – usually in the area of attachment – or loosening at the attachment points. 7 samples

133   were available in the D1 group, and 8 in each of the D2 and D3 groups.

134   The force-displacement behavior during uniaxial measurement was determined for the three depths.

135   The corresponding stress-strain data was calculated from the measurements (Figure 3). Besides the

136   typical viscous and nonlinear relationship, our results showed that the mechanical properties of the

137   stroma decreased with depth, with the anterior D1 group having the highest force, then the central

138   D2 layer, and the lowest in the posterior D3 stromal layer. The highest variability in stress was

139   observed in the D3 group (Figure 3). Statistically, D1 and D2 showed a significant difference in force

140   ($p < 0.001$), as did D2 and D3 ($p < 0.001$) and D1 and D3 ($p < 0.001$). An average maximum force of

141   0.22 N was observed in the D1 group, 0.18 N in the D2 group and 0.14 N in the D3 group at 10 % strain.

142   This corresponds to a decrease of 18 % mechanical strength in the central layer (D2) and a 36 % in the

143   posterior layer (D3), as compared to the anterior layer (D1).

144   The stress- strain data were used to calculate the tangent modulus at 2 %, 5 % and 10 % strain. The

145   average stress at 10 % strain was used to calculate the difference in mechanical strength between the

146   three layers. A linear decrease in mechanical properties was observed across depth. The tangent

147   moduli were evaluated at different strain levels (Figure 4). At 5 % strain, groups D2 and D3 showed no

148   significant difference ($p = 0.051$), but at 10 % this changed to a significant difference ($p < 0.001$). At all

149   strains, the tangent modulus was significantly higher at D1 than D2 and D3 ($p < 0.001$). We found no

150   correlation of tangent modulus with age or thickness.

151   Exponential fitting of stress-strain data showed good agreement with experimental data for all the

152   depths (Figure 3). Interestingly, the value of exponent B remains nearly constant across different

153   depths, implying that the mechanical properties between depths are primarily determined by the

154   linear parameter A over a strain range from 0% to 10% (Table 1). The relative change in corneal

155   stiffness between depths was quantified by calculating the normalized stiffness with respect to the

156   anterior depth. Since the exponential parameter B remains constant at all depths, this relationship is

157   nearly constant at each strain level. Furthermore, stiffness decreases linearly from the anterior to the

158   posterior. The central cornea has a stiffness of about 80% of the anterior stiffness, while the posterior

159   layer is 60% (Figure 5).

160

161   **3. DISCUSSION**

162   The objective of this study is to characterize the mechanical properties of the human corneal stroma

163   at different depths, corresponding to the anterior, central, and posterior cornea by uniaxial extension.

164   The study aims to understand the depth-dependent biomechanical behavior of the cornea under

165   tensile loading, which is one of the most relevant loading situation for physiological conditions (Kling

166   et al., 2020). While the physiological intraocular pressure is better represented by a biaxial setting,

167   uniaxial testing is a widely used method for estimating tensile mechanics. This study is the first to

168   characterize the depth-dependent biomechanics of the human cornea under tensile loading. It should

169   contribute to a better understanding of the biomechanical properties of the cornea and allow the

170   development of new treatment strategies for corneal diseases.

171   In this study, a linear decrease in tensile mechanical strength was observed across the depth of the

172   cornea. The central layer was found to be 18 % weaker than the anterior cornea and the posterior

173   cornea was found to be 38 % weaker than the anterior cornea.

174   Other depth-dependent mechanical characterizations found in the literature include shear (Petsche

175   et al., 2012; Sloan et al., 2014), compression (Ramirez-Garcia et al., 2018), cohesive tensile (Randleman

176   et al., 2008), and indentation (Labate et al., 2015). Direct comparison of measured properties is not

177   possible because the metric used to characterize the mechanical response is different for each test

178   method. Qualitatively, all these studies found significant stiffer properties for anterior cornea than the

179   posterior cornea. However, these studies report that the central stroma is mechanically similar to the

180   posterior cornea, which is different from our results, where significant differences in the mechanical

181   behavior were observed at all measurement depth – anterior, central, and posterior – with the

182   stiffness linearly decreasing across depth. This difference in analysis may be attributed to the type of

183   loading applied to samples in the different tests. The tensile strength of the collagen bundles is the

184   primary contributor to the uniaxial forces, which is orders of magnitude higher in tension than in

185   compression. As such, compression tests predominantly characterize the response of the stromal

186   matrix rather than the properties of the collagen fiber, which can explain these differences (Sun,

187   2021).

188   In this study, the posterior cornea was found to be 38% less stiff than the anterior cornea, which is in

189   a similar range to the depth dependent tensile mechanics of the porcine cornea (Nambiar et al., 2022).

190   The central layer was found to be 18% less stiff than the anterior cornea, which was different from

191   the trends in the porcine cornea that showed a similar mechanical strength of the central and anterior

192   layers (Nambiar et al., 2022). Comparing the results of this study with uniaxial measurements on full

193   thickness human corneal strips show that stresses of full thickness measurements are in the range of

194   D2-D3 groups of this study (Elsheikh, A. et al., 2008; Hoeltzel et al., 1992; Mahdian et al., 2021). The

195   deviations can be attributed to the depth dependence of the material and to differences in the test

196   setup, such as clamping and preconditioning. The parameters obtained by fitting the exponential

197   function indicate a more linear response of the tissue compared with the values published for inflation

198   experiments (Eliasy et al., 2019; Elsheikh et al., 2010). This difference could be due to the different

199   loading methods used in the two studies, especially since the inflation experiments reflect a

200   predominantly biaxial loading scenario. This comparison indicates that uniaxial tests should be

201   combined with biaxial loading to obtain a comprehensive description of the corneal mechanical

202   response.

203   Accurate quantification of the tensile strength in a depth-controlled manner is critical information that

204   is lacking in current numerical models developed to study various refractive interventions (Ariza-

205   Gracia et al., 2017; Pandolfi and Manganiello, 2006; Sinha Roy et al., 2014; Studer et al., 2010). Even

206   if the mechanical properties identified in this study corresponds to aged corneas, the trends of

207   reduction in strength quantified in this study can be reproduced for applications in the young cornea,

208   which is supported by imaging data and the other mechanical tests in literature (Labate et al., 2015;

209   Petsche et al., 2012; Ramirez-Garcia et al., 2018; Randleman et al., 2008; Sloan et al., 2014).

210   Looking at the ultrastructure of the human cornea, we see that collagen fibers of the anterior stroma

211   are randomly dispersed in the plane of the cornea and aligned along the curvature (Quantock et al.,

212   2007). This in-plane dispersion becomes preferentially oriented in the nasal-temporal and superior-

213   inferior directions with increasing depth, while preserving some level of isotropic scatter (Abass et al.,

214   2015; Quantock et al., 2007). However, the posterior cornea exhibits lower mechanical properties,

215   which seems contradictory because the fibers carry most of the load. This behavior could indicate

216   lower fiber density in the posterior cornea. The lower stiffness could also be due to a greater out-of-

217   plane dispersion of the fibers in the posterior cornea, resulting in a lower contribution of the fibers to

218   the tensile stress. It is plausible that a combination of these elements are at play.

219   This also makes the lack of orientation markers on the donor tissue a limitation of this study for the

220   posterior group (D3), and a possible explanation for the larger variability in the properties measured

221   in this group. Another reason for the larger variability observed in the mechanical measurements in

222   the posterior group could be related to fact the posterior stroma is more susceptible to swelling (Meek

223   et al., 2003; Wang et al., 2004), especially after removal of the DM. Although care was taken to

224   maintain the level of hydration of the specimens during testing, the corneas remained slightly swollen

225   when the specimens were cut from the cornea with the laser. This problem is common in ex vivo

226   mechanical testing. Although this may result in a slight underestimation of the measured stresses, the

227   trends and magnitude of the decrease in mechanical strength with depth remain valid. Another

228   simplification in this study is the assumption that the strips are flat, although the cornea has a

229   curvature. However, we suspect that the effect on the measured properties is small because of the

230   small dimensions of the specimens-particularly their thickness-and the fact that they flatten under

231   their own weight when attached to the experimental setup. Since the corneas were obtained from

232   transplant tissue, they were from elderly donors, which limits the measured properties to the elderly

233   population and prevents conclusions about age-dependent mechanical behavior. We found no

234   correlation of tangent modulus with age, which may be attributed to the limited age variation within

235   the measured samples.

236   This study contributes to the growing body of knowledge on the biomechanics of the human cornea

237   by quantifying the depth-dependent tensile biomechanics. This work also highlights the importance

238   of considering depth-dependent mechanical properties when planning and evaluating corneal

239   treatments. The results from this study could inform the development of better numerical models for

240   refractive interventions and improve our understanding of corneal diseases. The method by which

241   corneal stroma was derived in this study from DMEK surgical waste can be an important source of

242   corneal stroma for future research.

243   **FUNDING**

245

246 **REFERENCES**

247 Abass, A., Hayes, S., White, N., Sorensen, T., Meek, K.M., 2015. Transverse depth-dependent changes

248   in corneal collagen lamellar orientation and distribution. J. R. Soc. Interface 12.

249   https://doi.org/10.1098/rsif.2014.0717

250 Ariza-Gracia, M., Ortillés, Cristóbal, J., Rodríguez Matas, J.F., Calvo, B., 2017. A numerical-experimental

251   protocol to characterize corneal tissue with an application to predict astigmatic keratotomy

252   surgery. J. Mech. Behav. Biomed. Mater. 74, 304–314.

253   https://doi.org/10.1016/j.jmbbm.2017.06.017

254 Boschetti, F., Triacca, V., Spinelli, L., Pandolfi, A., 2012. Mechanical characterization of porcine

255   corneas. J. Biomech. Eng. 134, 1–9. https://doi.org/10.1115/1.4006089

256 Bunya, V.Y., Syed, Z.A., Puente, M.A., 2023. EyeWiki- American Academy of Ophtalmlology [WWW

257   Document]. URL https://eyewiki.aao.org/Corneal_Donation

258 Eliasy, A., Chen, K.-J., Vinciguerra, R., Lopes, B.T., Abass, A., Vinciguerra, P., Ambrósio Jr, R., Roberts,

259   C.J., Elsheikh, A., 2019. Determination of corneal biomechanical behavior in-vivo for healthy eyes

260   using CorVis ST tonometry: stress-strain index. Front. Bioeng. Biotechnol. 7, 105.

261 Elsheikh, A., Brown, M., Alhasso, D., Rama, P., Campanelli, M., Garway-Heath, D., 2008. Experimental

262   assessment of corneal anisotropy. J. Refract. Surg. Off. Publ. Int. Soc. Refract. Surg. 24.

263 Elsheikh, A., Alhasso, D., Rama, P., 2008. Biomechanical properties of human and porcine corneas.

264   Exp. Eye Res. 86, 783–790. https://doi.org/10.1016/j.exer.2008.02.006

265 Elsheikh, A., Geraghty, B., Rama, P., Campanelli, M., Meek, K.M., 2010. Characterization of age-related

266   variation in corneal biomechanical properties. J. R. Soc. Interface 7, 1475–1485.

267 Elsheikh, A., Kassem, W., Jones, S.W., 2011. Strain-rate sensitivity of porcine and ovine corneas. Acta

268   Bioeng. Biomech. 13.

269   Hamon, L., Daas, L., Mäurer, S., Weinstein, I., Quintin, A., Schulz, K., Langenbucher, A., Seitz, B., 2021.

270   Thickness and Curvature Changes of Human Corneal Grafts in Dextran-Containing Organ Culture

271   Medium   Before   Keratoplasty.   Cornea   40,   733–740.

272   https://doi.org/10.1097/ICO.0000000000002543

273   Hoeltzel, D.A., Altman, P., Buzard, K., Choe, K. Il, 1992. Strip extensiometry for comparison of the

274   mechanical response of bovine, rabbit, and human corneas. J. Biomech. Eng. 114, 202–215.

275   https://doi.org/10.1115/1.2891373

276   Kling, S., Khodadadi, H., Goksel, O., 2020. Optical Coherence Elastography-Based Corneal Strain

277   Imaging During Low-Amplitude Intraocular Pressure Modulation. Front. Bioeng. Biotechnol. 7.

278   https://doi.org/10.3389/fbioe.2019.00453

279   Labate, C., Lombardo, M., De Santo, M.P., Dias, J., Ziebarth, N.M., Lombardo, G., 2015. Multiscale

280   investigation of the depth-dependent mechanical anisotropy of the human corneal stroma.

281   Investig. Ophthalmol. Vis. Sci. 56, 4053–4060. https://doi.org/10.1167/iovs.15-16875

282   Mahdian, M., Seifzadeh, A., Mokhtarian, A., Doroodgar, F., 2021. Characterization of the transient

283   mechanical properties of human cornea tissue using the tensile test simulation. Mater. Today

284   Commun. 26, 102122. https://doi.org/10.1016/j.mtcomm.2021.102122

285   Meek, K.M., Leonard, D.W., Connon, C.J., Dennis, S., Khan, S., 2003. Transparency, swelling and

286   scarring in the corneal stroma. Eye 17, 927–936. https://doi.org/10.1038/sj.eye.6700574

287   Nambiar, M.H., Liechti, L., Müller, F., Bernau, W., Studer, H., Roy, A.S., Seiler, T.G., Büchler, P., 2022.

288   Orientation and depth dependent mechanical properties of the porcine cornea: Experiments and

289   parameter   identification.   Exp.   Eye   Res.   224,   109266.

290   https://doi.org/10.1016/j.exer.2022.109266

291   Pandolfi, A., Manganiello, F., 2006. A model for the human cornea: Constitutive formulation and

292   numerical analysis. Biomech. Model. Mechanobiol. 5, 237–246. https://doi.org/10.1007/s10237-

293   005-0014-x

294   Petsche, S.J., Chernyak, D., Martiz, J., Levenston, M.E., Pinsky, P.M., 2012. Depth-dependent

295   transverse shear properties of the human corneal stroma. Investig. Ophthalmol. Vis. Sci. 53, 873–

296   880. https://doi.org/10.1167/iovs.11-8611

297   Quantock, A.J., Boote, C., Young, R.D., Hayes, S., 2007. Small-angle fibre diffraction studies of corneal

298   matrix structure : a depth-profiled investigation of the human eye-bank cornea 335–340.

299   https://doi.org/10.1107/S0021889807005523

300   Ramirez-Garcia, M.A., Sloan, S.R., Nidenberg, B., Khalifa, Y.M., Buckley, M.R., 2018. Depth-Dependent

301   Out-of-Plane Young's Modulus of the Human Cornea. Curr. Eye Res. 43, 595–604.

302   https://doi.org/10.1080/02713683.2017.1411951

303   Randleman, J.B., Dawson, D.G., Grossniklaus, H.E., McCarey, B.E., Edelhauser, H.F., 2008. Depth-

304   dependent cohesive tensile strength in human donor corneas: Implications for refractive

305   surgery. J. Refract. Surg. 24, 20080101. https://doi.org/10.3928/1081597x-20080101-15

306   Roberts, C.J., 2016. Importance of accurately assessing biomechanics of the cornea. Curr. Opin.

307   Ophthalmol. 27, 285–291. https://doi.org/10.1097/ICU.0000000000000282

308   Sinha Roy, A., Dupps, W.J., Roberts, C.J., 2014. Comparison of biomechanical effects of small-incision

309   lenticule extraction and laser in situ keratomileusis: Finite-element analysis. J. Cataract Refract.

310   Surg. 40, 971–980. https://doi.org/10.1016/j.jcrs.2013.08.065

311   Sloan, S.R., Khalifa, Y.M., Buckley, M.R., 2014. The location- and depth-dependent mechanical

312   response of the human cornea under shear loading. Investig. Ophthalmol. Vis. Sci. 55, 7919–

313   7924. https://doi.org/10.1167/iovs.14-14997

314   Studer, H., Larrea, X., Riedwyl, H., Büchler, P., 2010. Biomechanical model of human cornea based on

315   stromal microstructure. J. Biomech. https://doi.org/10.1016/j.jbiomech.2009.11.021

316   Sun, B., 2021. The mechanics of fibrillar collagen extracellular matrix. Cell Reports Phys. Sci. 2.

317   https://doi.org/10.1016/j.xcrp.2021.100515

318   Wang, J., Simpson, T.L., Fonn, D., 2004. Objective measurements of corneal light-backscatter during

319   corneal swelling, by optical coherence tomography. Investig. Ophthalmol. Vis. Sci. 45, 3493–

320   3498. https://doi.org/10.1167/iovs.04-0096

321   Wolf, A.H., Welge-Lüen, U.C., Priglinger, S., Kook, D., Grueterich, M., Hartmann, K., Kampik, A.,

322   Neubauer, A.S., 2009. Optimizing the deswelling process of organ-cultured corneas. Cornea 28,

323   524–529. https://doi.org/10.1097/ICO.0B013E3181901DDE

324   Wollensak, G., Spoerl, E., Seiler, T., 2003. Stress-strain measurements of human and porcine corneas

325   after riboflavin-ultraviolet-A-induced cross-linking. J. Cataract Refract. Surg. 29, 1780–1785.

326   https://doi.org/10.1016/S0886-3350(03)00407-3

327

328

Depth	A (MPa)	B (-)	ε_0
D1	64.20 10^{-3}	25.28	11.19 10^{-3}
D2	47.41 10^{-3}	25.54	14.35 10^{-3}
D3	25.64 10^{-3}	26.74	22.37 10^{-3}

329   **Table 1:** The estimated parameters from the exponential fitting of the experimental stress strain data
330   showed a linear decrease in parameter 'A' while parameter 'B' remained relatively constant.
331   Parameter ε_0 was obtained to account for the prestress in the experimental condition at 0 strain.
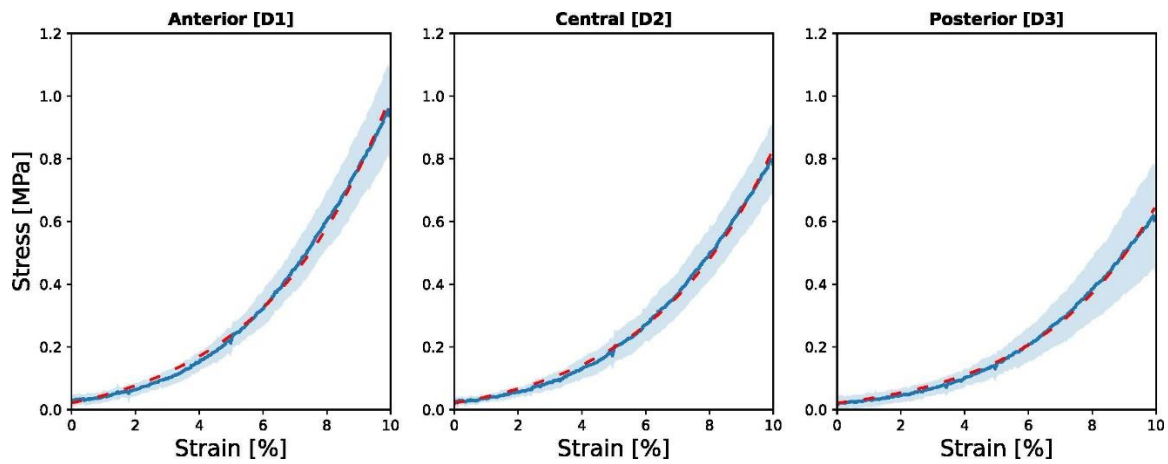
332

333
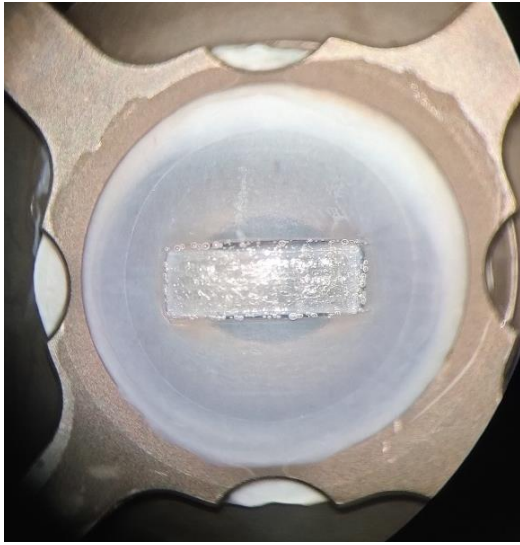
334

335   **Figure 1:** The cornea with scleral rim, clamped in an artificial chamber showing the strips cut out in
336   the mid corneal region.
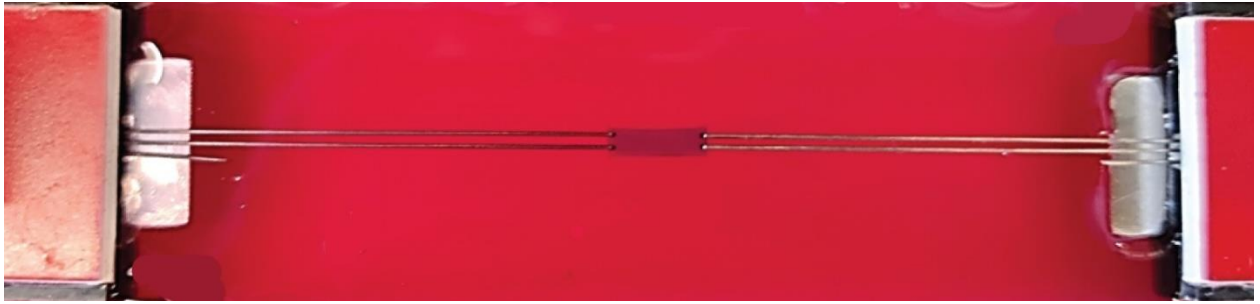
337

338 **Figure 2:** The corneal strip (6 x 2 x 0.15 mm) was tested under traction in a bath of MEM + 5%
339 dextran with BioRake attachments. Note that one of the tins has been cut on both sides to leave
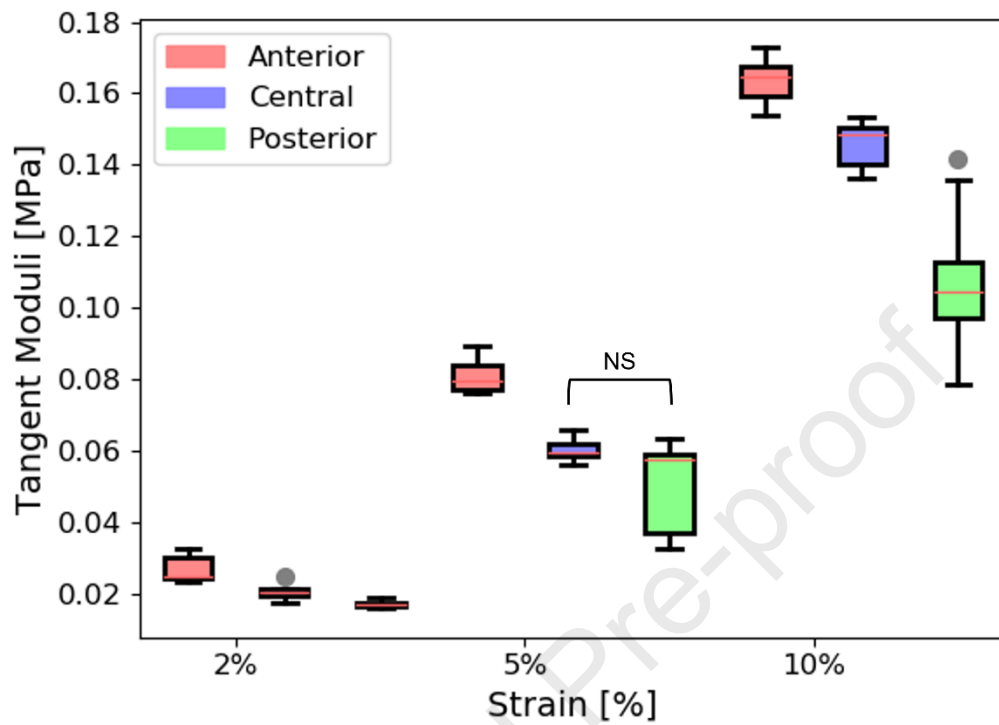340 only two for sample attachment.

341

342 **Figure 3:** The Stress-Strain reaction of the strips in the anterior (D1, n=7), central (D2, n=8) and
343 posterior (D3, n=8) groups. The solid blue line represents the mean stress, and the shaded region
344 represents the standard deviation. The dashed red line represents the exponential fit with equation
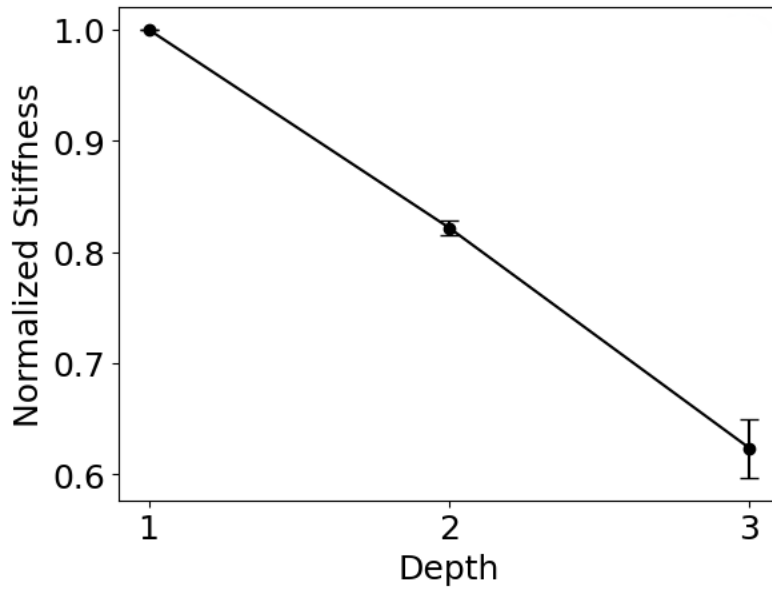345 1.

346

347

348

349

350

Figure 4: The tangent moduli in the anterior (D1, n=7), central (D2, n=8) and posterior (D3, n=8) groups, for 2%, 5% and 10 % strain. All groups except indicated (NS, $p = 0.051$) show a significant difference ($p < 0.05$).

354

355
356

357 **Figure 5:** The stiffness calculated based on the exponential fit at each depth was normalized with
358 respect to the stiffness of the anterior layer. This normalized stiffness ratio showed a linearly
359 decreasing stiffness from the anterior to the posterior part of the cornea.

Highlights

- Human cornea shows depth-dependent mechanical properties, with a linear decrease in tensile mechanical properties from the anterior to the posterior cornea.
- The tangent moduli at different strains show significant differences across the depth of the cornea.
- While full-thickness studies have been previously performed, this to the best of our knowledge, is the first depth-dependent analysis in uniaxial extension of the human cornea